Sintering and Foaming of Barium and Calcium Silicate Glass Powders

B. Agea Blanco[1+], C. Blaess[3+], S. Reinsch[2,] D. Brauer[3], R. Müller[2]
[1]Universitat Ramon Llull, IQS School of Engineering, Barcelona, Spain
[2]BAM Bundesanstalt für Materialforschung und -prüfung, Berlin, FRG,
Richard-Willstätter-Str. 11, 12489 Berlin, ralf.mueller@bam.de
[3]Otto-Schott-Institut für Materialforschung (OSIM), Jena, FRG
[+]On trainee leave at BAM

Abstract

Sintering and foaming of barium and calcium silicate glass powder compacts have been studied for different powder milling. Sintering was measured by means of heating microscopy backed up by XRD, DTA, Vacuum Hot Extraction (VHE) and electron microscopy. Foaming intensity strongly increased with decreasing glass particle size. Although powder compacts were uniaxially pressed and sintered in ambient air, foaming was affected by the milling atmosphere and most intensive for milling in CO_2. Conformingly, VHE studies revealed that foaming of fully sintered samples was mainly driven by CO_2, even for powders milled in technical air, Ar and N_2. Prolonged storage of air milled barium silicate glass powders in ambient air before pressing and sintering caused further increase of foaming intensity. These findings indicate that carbonaceous species are preferentially trapped to or close beneath the powder surface during milling and later storage. The temperature range of CO_2 degassing from fully sintered barium and calcium silicate glass powder compacts fits the temperature ranges of decomposition of $BaCO_3$ and $CaCO_3$ mix-milled with the respective barium and calcium silicate glass powders.

Key words: Barium and calcium silicate glass powders, sintering, degassing, foaming

Introduction

Numerous applications of sintered glasses, sintered glass-ceramics, glass matrix composites or glass bonded ceramics rely on crystallization stable or slowly crystallizing glass powders [1]. In these cases, low glass viscosity or prolonged annealing is often required for full densification of partially crystalline compacts and gases adsorbed to the powder surface, dissolved or encapsulated within the green compact porosity can be easily trapped by sintering thus preventing full densification and foaming [2], [3]. Regardless of their potential technological relevance and frequent occurrence, such phenomena have been rarely reported.

The present study is focused on the effect of glass powder preparation on foaming of sintered barium and calcium silicate glass powder compacts. Slow crystallizing barium silicate glasses are good candidates for SOFC sealants because of their high thermal expansion and appropriate process temperatures [4] [5] [6]. In this particular case, foaming is even less avoidable due to the sealant geometry, the viscous flow required for guaranteeing mechanically strong and gas tight sealing and due to the required long life-time at high operation temperature [7]. The calcium silicate glass powder under study is a promising candidate for bio glass applications, which require sufficient crystallization stability thus allowing manufacturing fibers or porous compounds [8].

In order to achieve better understanding of the effect of glass powder processing on sinter foaming phenomena, the barium and calcium silicate glass powders under study have been milled for different time and in different atmospheres including argon, nitrogen, ambient and technical air as well as carbon dioxide, uniaxially dry pressed and sintered in ambient air. Densification and foaming were studied by means of heating microscopy backed up by XRD, DTA, and optical and electron microscopies. Degassing was studied for green powder compacts by Vacuum Hot Extraction (VHE) coupled with mass spectroscopy.

Experimental

Samples

Barium disilicate glass (G1): The present study was made on a commercial barium disilicate glass with additions of B_2O_3, Al_2O_3 and ZnO used for SOFC sealing [9]. The purchased glass frit was sieved to <2mm and 15 min *pre-milled* in air using a planetary ball mill (Fritsch Pulverisette 5, Fritsch, Idar-Oberstein, Germany; 500ml, Al_2O_3 jars). Afterwards, a mechanical sieve (Analysette 3 PRO, Fritsch, Idar-Oberstein, Germany) was used to narrow the particle size distribution to 40-250 µm.

Milling in controlled atmosphere was performed in a smaller planetary ball mill (Planetary micro mill Pulverisette 7, Fritsch, Idar-Oberstein, Germany, 25 ml corundum jars). Controlled milling atmosphere was maintained with gas tight sealing rings. Sealed jars were filled with 4 corundum balls (∅ ≈ 12 mm) and 8 g of pre-milled glass powder, evacuated to < 20 mbar, and re-filled with CO_2, N_2, and technical Air (99.99% purity, Air Liquide™, Germany) to 10^5 Pa. Evacuation and re-filling was repeated five times to minimize the amount of residual ambient air. A liquid nitrogen trap was used to increase N_2 purity. Milling was stopped for 30 min after each 15 min milling step preventing overheat. After milling, the powder was stored in closed HDPE boxes.

The *calcium silicate glass G2* ($45SiO_2 \cdot 2P_2O_5 \cdot 36CaO \cdot 7Na_2O \cdot 7K_2O \cdot 3CaF$, mol% batch) was melted in a Pt crucible, fined for 1 h at 1350°C and fritted in water. Since this glass is prone to corrosive attack of water, 10 min milling of fine powders was performed in isopropanol (20 g glass, 25 ml isopropanol) using 80 ml zirconium jars with 10 zirconium balls each. Alternatively, the glass frit was crushed in a steel mortar and sieved to different particle size fractions. G2 Milling in CO_2 atmosphere was performed as described above for G1 but starting with the 315-3150 µm powder fraction. *Cylindrical powder compacts* were uniaxially pressed in ambient air without organic aids (G1: 60 MPa, Ø ≈ 5 mm, h ≈ 2 mm, m ≈ 0.1 g; G2: 50 MPa, Ø ≈ 5 mm, h ≈ 5 mm, m ≈ 0.1 g). Gas release studies were performed on likewise pressed powder compacts cut to small pieces of 10 mg.

Methods

Glass viscosity, η_G, was measured with rotational viscometry (VT550, Haake, Erlangen, Germany) for $\eta < 10^5$ Pa s. The glass transition temperature of G1 (T_g = 649 ± 3°C) was determined with a horizontal dilatometer (404 E, Netzsch, Selb, Germany). Obtained G1 viscosity data in Pa s and °C could be approximated with $\log\eta$ = -2.77+2644/(T-480) (G1) and -4.00 +3547/(T-359) (G2) within $\Delta \log\eta \approx \pm 0.02$ accuracy. T_g = 540 ± 5°C of G2 was obtained by DTA. *Glass density* (ρ_{G1} = 3.61 g/cm^3, ρ_{G2} =2.76 g/cm^3) was measured by means of Archimedes' principle. A Mastersizer 2000 (Malvern Instruments, Wocestershire, U.K.) was used for *particle size* measurement. Particle agglomeration was minimized by diluting ≈ 10 mg of glass powder in a 0.003 M $Na_4P_2O_7$ solution and ultra-sonic treatments (1-5 min).

Shrinkage of cylinder-shaped powder compacts during heating at 5 K/min (G1) and 10 K/min (G2) was examined using a heating microscope (Leitz, Wetzlar, Germany) with optical data acquisition (Hesse Prüftechnik, Osterode, Germany). The *bulk density* of green and sintered specimens was obtained from their sample geometry and weight.

The *microstructure* of powder compacts heated to selected temperatures and quenched in air was studied from polished cross-sections by means of environmental scanning electron microscopy (ESEM-FEG, Philips-XL 30, Eindhoven, Netherlands), or by an optical microscope (JENAPOL, Carl Zeiss Jena, Jena, Germany). Green powder compacts were infiltrated with synthetic resin for preparing cross sections.

Differential thermal analysis (DTA/DTG) was performed in air at 5 K/min (G1) and 10 K/min (G2) using ≈ 25 mg samples and Pt-crucibles (TAG24, Setaram, Caluire, France). $BaCO_3$/G1 and $CaCO_3$/G2 mix-milling was done for 5min in ambient air ($BaCO_3$: Solvay Barium Strontium GmbH, Bad-Hönningen, FRG; $CaCO_3$: Merck, Darmstadt, FRG; glass powders < 72 µm). *Porosity* was measured by image analysis of optical micrographs, using the software Image C (Aquinto AG, Berlin, Germany).

Crystallization was studied by means of X-ray diffraction (Philips PW 1710, Eindhoven, Netherlands) using copper K_α with λ = 1.5418 Å, in Bragg-Brentano symmetry. Data were collected for 2θ = 5°- 80° in steps of 0.02°/s. Diffraction patterns were analyzed using the software EVA 15.1 (Bruker-AXS, Karlsruhe, Germany) and compared to JCPDS database (JCPDS, 2009, International Center for Diffraction Data).

Gas release from green and sintered powder compacts was studied by means of Vacuum Hot Extraction (*VHE*) with mass spectrometer evolved gas detection (QMA4005, Balzers Instruments, Liechtenstein, Germany). VHE analysis were performed in vacuum (10^{-4} - 10^{-5} mbar) during heating at 20 K/min using the MID (multiple ion detection) mode [10].

Results

Glass G1: Fig. 1 shows the sintering and foaming of barium silicate glass powders (G1) milled in ambient air for different milling time. Sintering occurs between 700°C and 760°C. As expected, sintering onset decreases and maximum shrinkage increases with decreasing particle size. For 60 min milling (D_{90} = 25µm), sintering starts at 690°C, ≈ 40K above T_g at 649°C. Beyond maximum densification, progressive foaming is evident strongly promoted by prolonged milling.

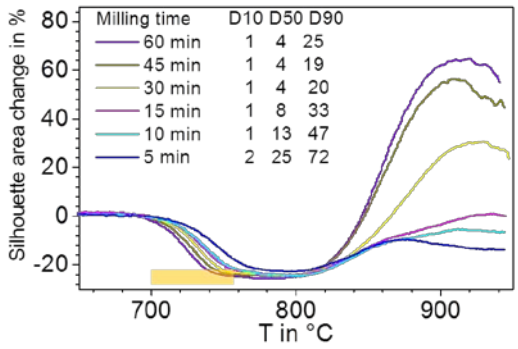

Fig. 1: Sintering and foaming of G1 powder compacts for different milling time versus temperature (5K/min)

Fig. 2 shows shrinkage and foaming of G1 glass powders 15 min milled in different atmosphere. Sinter shrinkage maximum occurs at 760-800°C beyond which progressive foaming occurs. This foaming is most pronounced for milling in CO_2 where it already starts at ≈ 760°C. In contrast, the smallest foaming effect is evident for milling in N_2 and Ar. Specific powder surface data calculated from experimental particle size distribution were found to be (m^2/g) 0.45, 0.35, 0.39, and 0.39 for technical air, N_2, Ar, and CO_2, respectively.

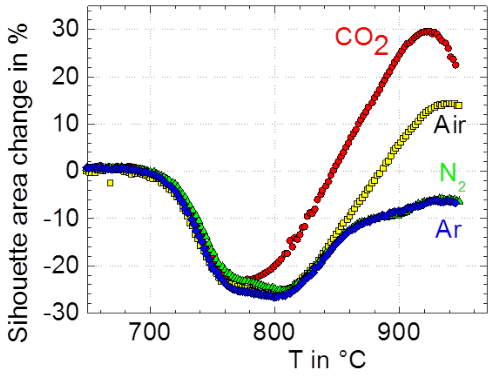

Fig. 2: Sintering and foaming of G1 glass powder compacts for different milling atmosphere versus temperature (5 K/min).

It is interesting to note that foaming for 15 min milling in ambient air (Fig. 1) is less pronounced than that for 15 min milling in technical air (Fig. 2) even though the attained specific surface in ambient air (0.54 m^2/g) is larger than that obtained for technical air (0.45 m^2/g).

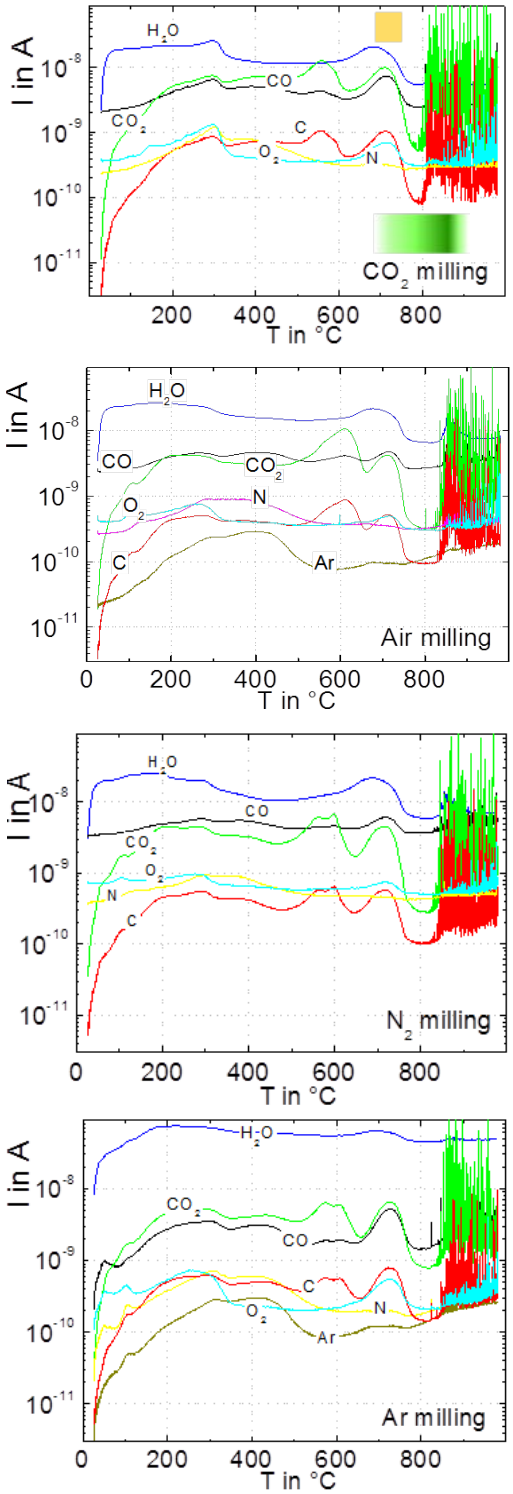

Fig. 3: Degassing of G1 green powder compacts (20K/min) for different milling atmosphere. Degassing activity is presented in terms of respective ion currents, *I*.

Fig. 3 shows VHE degassing of green powder compacts for milling in different atmosphere. At T < 800°C (onset of foaming), H_2O is the most prominent degassing species. Degassing of surface adsorbed water causes broad degassing peaks between 100°C and ≈ 400°C [10]. Water degassing is newly accelerated approaching T_g ≈ 649°C and strongly decreased by sintering > 700°C (yellow bar). This observation indicates that degassing is not fully exhausted but delayed by sintering. The second most intensive degassing < 800°C is that of CO_2 and its cracking fragments (CO, C).

During foaming (spikes > 800°C), however, degassing is dominated by CO_2. This finding indicates that CO_2 degassing is less exhausted below full sintering than that of all other volatiles. In contrast to CO_2, Ar and N_2 did not significantly contribute to foaming even for the powders milled in these atmospheres. Confirming Fig. 2, CO_2 milled powder shows the most intensive degassing during foaming.

Since it might be delayed by sintering, the degassing mechanism at ≈ 650 - 800°C is a potential source of foaming. In order to check whether this degassing might reflect the decomposition of $BaCO_3$ precipitates or similar structural sites within the glass, G1 glass powders (crushed to < 200µm and 5min milled in ambient air to < 72 µm) were 5 min mix-milled with $BaCO_3$ powders (< 45 µm, Solvay Barium Strontium GmbH, Bad-Hönningen, FRG) to equal mass fractions and measured by DTG. Fig. 4 (red curve) shows that this mix-milling step reduced the $BaCO_3$ decomposition temperature by ≈ 300K and that the maximum decomposition temperature of about 840°C nicely correlates to the foaming onset in Fig. 3

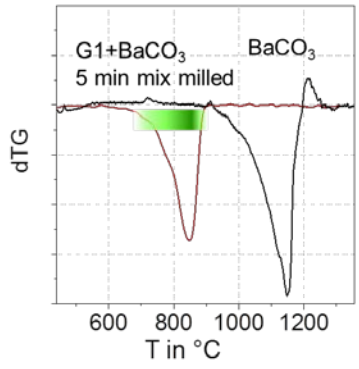

Fig. 4: DTG of $BaCO_3$ powder and $BaCO_3$ 5min mix-milled with G1 glass powder

In order to check potential gas uptake after milling, 15 min ambient air milled G1 glass powders were stored in closed HDPE boxes before pressing and sintering. Respective sintering and foaming curves are shown in Fig. 5 clearly indicating that gas uptake during storage might substantially contribute to foaming. A similar storage experiment was performed on 1h ambient air milled G1 glass powders (not shown). Despite a significant increase of foaming intensity for this 1h milling regime, it was found that 3 and 4 day storage did not result in different foaming. This finding indicates a saturation level of this phenomenon.

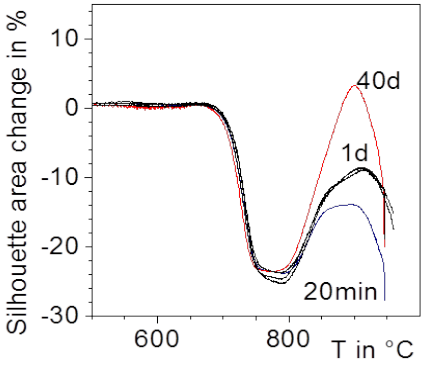

Fig. 5: Sintering and foaming of G1 glass powder compacts for 15 min milling in ambient air and prolonged storage versus temperature (5K/min)

Glass G2: Fig. 6 presents a DTA curve of G2 glass powders 10 min milled in isopropanol (D < 24µm). In contrast to G1, which does not crystallize during the thermal treatments applied here, glass G2 undergoes DTA detectable crystallization (T_{C1}, T_{C2}) after sintering (shoulder between 600°C and 660°C, yellow bar) and crystal melting is indicated by endothermic peaks (T_{M1}, T_{M2}).T_g is indicated at 540°C. Due to EDX (ESEM) crystals may be attributed to $Na_2Ca_4(PO_4)_2SiO_4$, which also occurs for the well-known bio glass 45S5® [11].

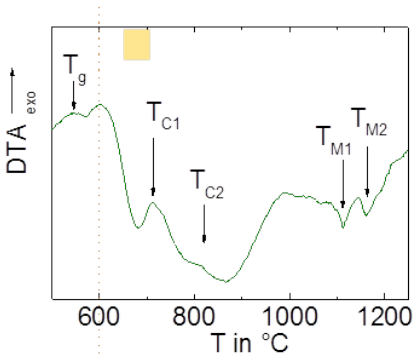

Fig. 6: DTA curve for G2 glass powder (<24 µm, milling in isopropanol, 10K/min).

Sintering and foaming of G2 glass powders is shown by Fig. 7. Due to its lower T_g, sintering starts ≈ 100K below that of G1 glass powders of similar particle size. The increase in shrinkage with decreasing particle size reflects the

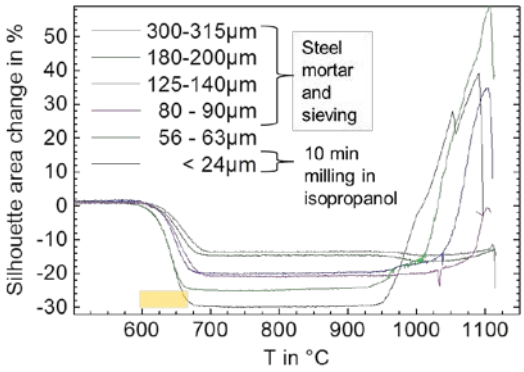

Fig. 7: Sintering and foaming of G2 glass powder compacts versus temperature (10K/min)

respective decrease in green density of pressed powder compacts. As for G1, G2 glass powder compacts undergo substantial foaming. This effect is evident both for dry crushing in a steel mortar and milling in isopropanol. Fig. 8 shows that degassing after densification (> 650°C, yellow bar) is dominated by CO_2 and its cracking fragments. H_2O does not much contribute to foaming. Fig. 9 compares bulk and milled G2 glass samples showing that degassing of powders is more intense. This finding again indicates that foaming gas is trapped at or near to the powder surface. Whereas this effect is most striking < 600°C (desorption), it also holds for foaming > 900°C. Only few degassing spikes hint on partial foaming from the glass bulk ($CaCO_3$ raw materials were used for glass melting).

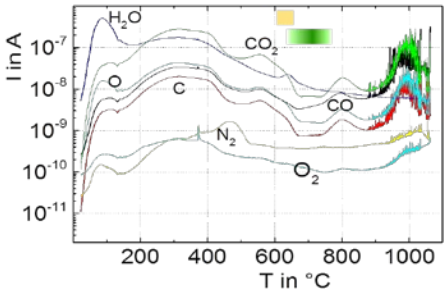

Fig. 8: Degassing of G2 powders (< 24µm, 20K/min). See Fig. 6 and Fig. 12 for bars.

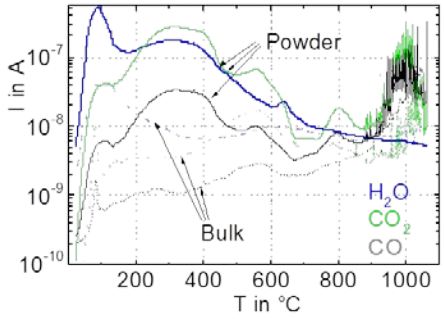

Fig. 9: Degassing of bulk (> 1mm) and powdered (< 24 µm) G2 glass (20K/min)

In contrast to G1 glass powders (Fig. 1, Fig. 2), however, foaming induced swelling (silhouette area increase) is delayed by more than 200K above densification. For the powder < 24 µm, swelling starts at 940°C (Fig. 7), which is slightly above the onset of bubble bursting in vacuum at ≈ 880°C (Fig. 8, Fig. 9). This finding indicates that the effective compact viscosity now enables the growth and bursting of large gas bubbles causing single spikes. Large bubble bursting is also indicated by sharp dips at ≈ 1000°C and 1040°C in Fig. 7. The marked drop of silhouette area > 1100°C coincides with the melting temperatures shown in Fig. 6.

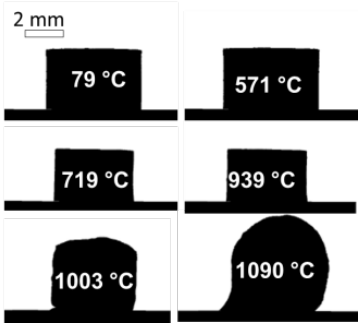

Fig. 10: Silhouettes of G2 glass powder compacts during heating at 10 K/min (< 24 µm)

Between densification and blowing (≈ 700°C - 900°C), the silhouette area in Fig. 7 and the cylinder shape of the samples (Fig. 10) remain constant. Nevertheless, smooth degassing is evident between 750 and 860°C in Fig. 8 and Fig. 9.

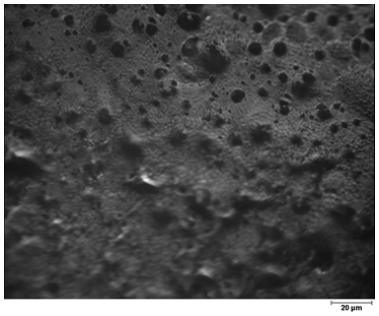

Fig. 11: Incident light micrograph of a G2 powder compact (< 24 µm) heated to 760°C

Optical microscopy (Fig. 11) revealed a non-regular and porous surface of sintered compacts within this temperature range indicating continuous degassing from partially crystalline samples kept in shape by their large effective compact viscosity. The small size and large number of simultaneously bursting bubbles may explain the appearance of a smooth degassing peak in Fig. 8 and Fig. 9. Cross sectional micrographs (not shown) indicate that the former surface region of glass particles could be

altered by corrosion or crystallization phenomena. In case of a reduced viscosity of this region, gas diffusion and bubble formation can proceed in this region even in case of powder compacts with large effective bulk viscosity. The decrease of this degassing activity above 800°C might be a result of gas exhaustion from this region or could be caused by progressive compact homogenization via diffusion.

The onset of this degassing mechanism at ≈ 730°C is close to the maximum decomposition temperature of $CaCO_3$ powders mix-milled with G2 glass powder at 720°C (Fig. 12). In contrast to G1/$BaCO_3$ however, mix-milling did not cause any substantial decrease of decomposition temperature.

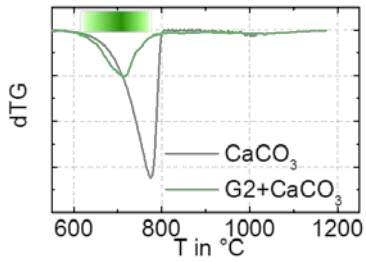

Fig. 12: DTG (10K/min) of $CaCO_3$ and $CaCO_3$ 5 min mix-milled with G2 glass powder

Discussion

Results given above can be explained in terms of a hypothesis suggested by Kalinkin [12]. The author reported extensive carbonization of silicate minerals during planetary ball milling in CO_2 atmosphere up to 12wt% for 30 min milling (10^5Pa CO_2, 40g centrifugal factor). Whereas no carbonate crystals could be detected after this milling procedure by XRD and the initial diffraction patterns of the silicate mineral fully disappeared, two IR peaks at 1410 and 1540 cm^{-1} indicate CO_3^{2-} dissolved to the XRD amorphous silicate mineral [13]. IR spectroscopic data were similar to finely ground glass obtained by quenching of silicate melt wherein CO_2 was dissolved at magma state conditions (1800 - 2000K, 1 - 2 GPa) [13], [14].

According to these findings it seems reasonable to assume, that glass powder milling can cause a thin surface layer where mechanical activation has caused structural defects, voids and micro cracks. Ongoing milling could even cause re-agglomeration of fine particles to the surface of bigger ones making up a re-solidified micro porous surface layer.

This layer tends to relax both its increased volume and surface energy. At low temperature ($T \ll T_g$), during milling or later storage, surface energy can be reduced by gas adsorption.

This process will establish a competitive adsorption – desorption equilibrium among different gas species present in the ambient process atmosphere. Since CO_2 was reported to show particular strong reactivity with freshly broken glass surfaces by Baptist [15], and due to the well-known affinity of water to the glass surface it seems plausible, that surface desorption measured by VHE (Fig. 3, Fig. 8, Fig. 9) is dominated by these species. It also explains the strong effect of milling in CO_2 on foaming. The kinetic character of such phenomena could explain the additional gas uptake after 15 min milling in air (Fig. 5), whereas no additional gas uptake was seen after 1h milling in CO_2 and 3 days storage in air.

As the sample is heated up, progressive bulk relaxation phenomena can occur within the structurally disturbed, micro porous surface layer of glass particles. This process can include healing of micro cracks and encapsulation of herein trapped gas species. In a sense, this process might be treated as some kind of “pre-sintering”, in which pressure assisted gas dissolution can occur. According to the reasons mentioned above, H_2O and CO_2 seem to be most prone to such wise dissolution phenomena if “pre-sintering” occurs above the typical range of physical surface desorption (>600°C in Fig. 3, see N_2 or Ar). This situation may not hold, however, for low melting glasses of lower glass transition temperature, where other gases might be entrapped as well.

As the most interesting consequence of this situation, degassing now requires both, (i) sufficient diffusion rate of dissolved species and, for chemical dissolution, (ii) the decomposition of related structural sites. As a consequence, degassing is retarded to temperatures close to T_g and volatile species are more easy trapped by sintering. Furthermore, as dissolved water is well known to decrease viscosity, it seems plausible that water can more easily escape from the powder near surface layer before being trapped by sintering. In this sense, it is understandable, why water much less contributes to foaming than CO_2 and why 15 min milling in ambient air caused less pronounced foaming than 15 min milling in technical air (Fig. 1, Fig. 5) regardless of the larger specific surface (0,54 versus 0,45 g/m^2) attained for milling in ambient air.

Fig. 4 and Fig. 12 show that the maximum decomposition rates of $BaCO_3$ and $CaCO_3$ mix-milled with G1 and G2 glass powders at 840°C and 720°C, respectively, occurs ≈ 40K above the respective densification temperatures at 800°C and 680°C. Both decomposition temperatures also coincide with the onset tempera-

tures of degassing after densification causing bursting spikes (Fig. 3, G1) and smooth degassing between 750 und 860°C (Fig. 8, G2). Although no strict evidence is given, this finding indicates that CO_2 is predominantly dissolved as CO_3^{2-}. Further systematic studies, however, are needed to clarify such questions.

Conclusion

For the barium and calcium silicate glasses under study (G1, G2), foaming intensity was strongly increased with decreased glass particle size. This finding gives clear evidence that the mayor source of foaming of fine powders is trapped at the powder surface or dissolved within a thin surface near layer.

Progressive gas uptake after G1 glass milling in ambient air indicates that gas uptake may be considered as part of relaxation of the mechanically activated glass surface.

Degassing studies on both glasses revealed that foaming is mainly driven by CO_2, even for milling in Ar and N_2 (G1) or for dry crushing in a steel mortar (G2). This finding indicates pronounced selective CO_2 uptake during crushing, milling or later processing. Although H_2O dominates the degassing of powder compacts below the sintering onset for both glasses, it does not significantly (G2) or only partially (G1) contribute to the foaming of densified powder compacts.

The temperature range of CO_2 degassing from densified powder compacts was found to roughly coincide with the decomposition range of $BaCO_3$ and $CaCO_3$ powders mix-milled with G1 and G2 glass powders, respectively.

The occurrence of crystallization after densification of G2 glass powder compacts was found to substantially retard the onset of degassing induced sample swelling, which can be easily explained in terms of the increased effective compact viscosity.

Acknowledgements

ERASMUS support for the Bachelor trainee leave of the first author is much appreciated. The authors thank M. Gaber (VHE), I. Feldmann (ESEM), R. Schadrack (dilatometrie), and R. Sojref (milling) for technical help and valuable discussions.

References

[1] R. Müller and S. Reinsch, "Viscous Phase Silicate Processing," pp. 75 - 144. In *Processing Approaches for Ceramics and Composites*. Edited by N. Bansal and A. R. Boccaccini. John Wiley & Sons, Hoboken, New Jersey, U.S.A, 2012.

[2] B. Agea Blanco, "Sintering and bloating phenomena of barium disilicate glass powders," bachelor Thesis, IQS, Universitat Ramon Llull, Barcelona, Spain (2013).

[3] R. Muller, R. Meszaros, B. Peplinski, S. Reinsch, M. Eberstein, W. A. Schiller, and J. Deubener, "Dissolution of Alumina, Sintering, and Crystallization in Glass Ceramic Composites for LTCC," *Journal of the American Ceramic Society,* 92[8] 1703-1708 (2009).

[4] J. W. Fergus, "Sealants for solid oxide fuel cells," *Journal of Power Sources,* 147[1-2] 46-57 (2005).

[5] S. M. Gross, T. Koppitz, J. Remmel, and U. Reisgen, "Glass-ceramic materials of the system BaO-CaO-SiO_2 as sealants for SOFC applications," pp. 239-245 in *Proceedings of the Ceramic Engineering and Science Proceedings*. Edited by N. P. Bansal, D. Zhu, andW. M. Kriven. 2005.

[6] R. N. Singh, "Sealing technology for solid oxide fuel cells (SOFC)," *International Journal of Applied Ceramic Technology,* 4[2] 134-144 (2007).

[7] T. Schwickert, R. Sievering, P. Geasee, and R. Conradt, "Glass-ceramic materials as sealants for SOFC applications," *Materialwissenschaft und Werkstofftechnik,* 33[6] 363-366 (2002).

[8] D. Groh, F. Doehler, and D. S. Brauer, "Bioactive glasses with improved processing. Part 1. Thermal properties, ion release and apatite formation," *Acta Biomaterialia,* 10[10] 4465-4473 (2014).

[9] Glaslotpulver Typ K01 (Product-ID 6.FC0700.DL.00000) supplied by Kerafol Keramische Folien GmbH Eschenbach FRG.

[10] R. Muller, P. Gottschling, and M. Gaber, "Water concentration and diffusivity in silicates obtained by vacuum extraction," *Glass Science and Technology,* 78[2] 76-89 (2005).

[11] X. Chatzistavrou, T. Zorba, E. Kontonasaki, K. Chrissafis, P. Koidis, and K. M. Paraskevopoulos, "Following bioactive glass behavior beyond melting temperature by thermaland optical methods," *Physica Status Solidi a-Applied Research,* 201[5] 944-951 (2004).

[12] A. Kalinkin, "Kinetics of carbon dioxide mechanosorption by Ca-containing silicates," *Journal of Thermal Analysis and Calorimetry,* 95[1] 105-110 (2009).

[13] E. V. Kalinkina, A. M. Kalinkin, W. Forsling, and V. N. Makarov, "Sorption of atmospheric carbon dioxide and structural changes of Ca and Mg silicate minerals during grinding - I. Diopside," *International Journal of Mineral Processing,* 61[4] 273-288 (2001).

[14] G. Fine and E. Stolper, "Dissolved carbon dioxide in basaltic glasses: concentrations and speciation," *Earth and Planetary Science Letters,* 76[3–4] 263-278 (1986).

[15] R. Baptist and F. Levy, "Carbon-Dioxide Adsorption on Glass," *Vacuum,* 43[3] 213-214 (1992).